

HI KINEMATICS IN A MASSIVE SPIRAL GALAXY AT $Z=0.89$

L.V.E. KOOPMANS

Space Telescope Science Institute, 3700 San Martin Drive, Baltimore, MD 21218, USA

A.G. DE BRUYN

NFRA-ASTRON, P.O. Box 2, Dwingeloo 9700 AA, The Netherlands
Kapteyn Astronomical Institute P.O. Box 800, NL-9700 AV Groningen, Netherlands*Draft version February 2, 2008*

ABSTRACT

We present a kinematic model of the neutral-hydrogen in the spiral galaxy of the lens system PKS1830–211, based on a Multi Element Radio-Linked Interferometer (MERLIN) 1.4-GHz radio map and the integrated and redshifted 21-cm hydrogen absorption-line profile as measured with the Westerbork Synthesis Radio Telescope (WSRT). Degeneracies in the models do not allow a unique determination of the kinematic center and forthcoming deeper Hubble Space Telescope observations with the Advanced Camera for Surveys (ACS) are required to break this degeneracy. Even so, we measure the inclination of the hydrogen disk: $i = (17 - 32)^\circ$, indicating a close-to face-on spiral galaxy. The optical depth increases with radius over the extent of the Einstein ring, suggesting HI depletion towards the lens center. The latter could be due to star formation or conversion of HI in to molecular hydrogen because of a higher metallicity/dust content in the galaxy center. The neutral hydrogen optical depth gives $N_{\text{HI}} = 2 \times 10^{21} \text{ cm}^{-2}$ at $r = 5.0 h_{70}^{-1} \text{ kpc}$ in the disk ($T_s = 100 \text{ K}$), comparable to local spiral galaxies. Our study shows that planned new radio telescopes (i.e. ALMA, LOFAR and SKA) – which will discover large numbers of similar lens systems – are powerful new tools to probe the internal structure, kinematics and evolution of spiral galaxies in detail to $z \gtrsim 1$, as well as their neutral-hydrogen (and molecular) content, thereby complementing studies of HI emission from spirals at $z \lesssim 1$ and damped Ly- α systems to $z \gg 1$.

Subject headings: gravitational lensing — galaxies: structure — ISM: kinematics and dynamics — line: profiles

1. INTRODUCTION

The gravitational lens PKS 1830–211 (e.g. Pramesh Rao & Subrahmanyam 1988; Subrahmanyam et al. 1990) is the brightest known radio lens in the sky. The source at $z=2.51$ (Lidman et al. 1999) is extended and lensed into an Einstein ring (e.g. Jauncey et al. 1991) by a high-redshift spiral galaxy at $z = 0.89$ (Wiklind & Combes 1996; Gerin et al. 1997; Mathur & Nair 1997; Chengalur, de Bruyn & Narasimha 1999). In addition, a time-delay of 26 ± 5 days between the two images of the lensed core has been measured (Lovell et al. 1998; see also Wiklind & Alloin 2002). New monitoring data in hand is expected to yield an improved measurement of this delay (J. Winn, private communications). The structure of the Einstein ring can be used to place constraints on the mass distribution of the lens (Kochanek & Narayan 1992; Nair, Narasimha, & Rao 1993; Wiklind & Alloin 2002). Were it not that PKS 1830–211 is seen through the Galactic disk (i.e. $l = +12^\circ$, $b = -5^\circ$) – leading to considerable optical extinction ($A_I = 0.8 \text{ mag}$) and a field crowded by stars (e.g. Winn et al. 2002; Courbin et al. 2002) – this lens system would be well-suited to determine the Hubble Constant. Due to the severe extinction it has proven difficult to precisely determine the center of the lens galaxy. A number of mutually inconsistent lens centers have been published over the years (e.g. Kochanek & Narayan 1992; Nair et al. 1993; Lehar et al. 2000). Most recently, using the same HST observations, two different interpretations of the lens center were published (Winn et al. 2002; Courbin et al.

2002). The inability to measure the lens center with the currently available observations severely limits the use of PKS 1830–211 to determine H_0 . Forthcoming HST–ACS observations, however, will be able to settle this question.

Besides being interesting because of H_0 , the lens galaxy in PKS 1830–211 is the highest-redshift spiral lens galaxy known. The brightness of the lensed source has allowed a unique study of the molecular (e.g. CO and OH) and atomic (i.e. HI) interstellar medium (ISM) content (Wiklind & Combes 1996; Gerin et al. 1997; Mathur & Nair 1997; Chengalur, de Bruyn & Narasimha 1999) in a spiral galaxy as seen $\approx 8 h_{70}^{-1} \text{ Gyr}$ ago. Although only a single galaxy, it provides a test case for similar systems anticipated to be discovered with planned instruments such as ALMA, LOFAR and SKA.

The time base-line covered by these galaxies provide enough leverage to study the evolution of the mass-distribution and ISM of spiral galaxies in the redshift-regime where most of their evolution is expected to occur and also connects up to studies of damped Ly- α systems (e.g. Kauffmann 1996; Mo, Mao & White 1998).

In this letter, we make a first attempt to model the kinematics of HI in this high-redshift spiral galaxy, improving upon a previous more simple analysis by Chengalur et al. (1999). One of the initial aims, i.e. the determination of an independent kinematic lens center, has proven too difficult given the current data, but constraints on the radial distribution of HI, its column density and kinematics are obtained.

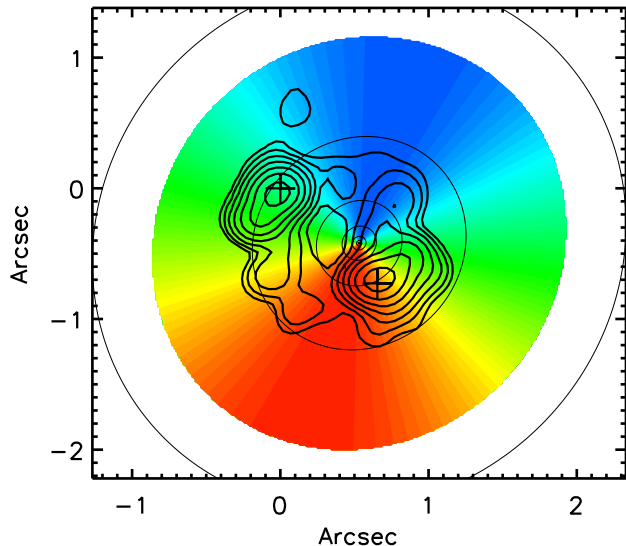


FIG. 1.— The MERLIN 1.4-GHz continuum maps of PKS 1830–211 (North is up and East is left). Contours start at 25 mJy/beam and increase by factors of two. Overplotted is the best-fit kinematic model for the lens center of Nair et al. (1993). The two crosses indicate the lensed cores A (NE) and B (SW). The thin elliptical contours indicate constant optical depth increasing by factors of 2 outward. The optical depth contour passing through image B has $\tau=0.064$.

2. MERLIN & WSRT OBSERVATIONS

MERLIN long-track observations of PKS1830–211 were obtained at 1.4, 1.7 and 4.9 GHz on, respectively, March 26, 25 and 8 in 1999. The data were flux and phase calibrated at the telescope. We subsequently map the data using DIFMAP (Shepherd 1997) following standard procedures, but perform additional self-calibration in the case that small phase and flux calibration errors are still present in the data. The resulting map at 1.4 GHz is shown in Fig.1. All maps will be presented in more detail in forthcoming publications. The 1.4-GHz map is used as a representation of the surface brightness distribution against which we observe the HI distribution in the lens galaxy. We use it to calculate the HI absorption line. We note that absorption really occurs at $1.42/(1+z_l) = 0.75$ GHz, for which we do not have a radio map. However, the difference between the 1.4 and 1.7 GHz maps are small and we expect the radio map at 0.75 GHz to be quite similar to that at 1.4 GHz. Using the 1.7 and 1.4 GHz radio maps to construct an estimated 0.75-GHz radio map is difficult given the different UV sampling. We therefore opt to solely use the 1.4-GHz map.

The multi-frequency frontends of the WSRT were used to obtain a high signal-to-noise profile of the HI absorption line at a frequency of 753 MHz. Compared to the previous observations of Chengalur et al. (1999) the data have superior spectral resolution and wider bandwidth as well as a better spectral baseline. In total we obtained 5.5 hrs of data on PKS1830–211 with 12 MFFE's on October 25, 1998. A backend bandwidth of 2.5 MHz was

used with 256 channels, giving 3.9 km s^{-1} per channel. The data were Hanning smoothed to give a resolution at halfwidth of 7.9 km s^{-1} . The resulting normalized line profile is shown in Fig.2. Errors are estimated from the rms scatter between channels at the baseline level well away from the line profile.

3. KINEMATIC MODEL

We model the HI absorption line, assuming a thin axisymmetric HI disk with an optical depth $\tau(r) = \tau_0 \times (r/r_0)^\gamma$. The disk has a kinematic center (x_k, y_k) on the sky, an inclination i and position angle θ (measured north to east on the sky). The HI gas has a constant circular velocity v_c , as expected for an isothermal mass distribution of the lens galaxy and a systemic velocity v_s . The latter allows for a small velocity difference with respect to the redshift determined from molecular lines. For each surface brightness element $\Sigma_v(\vec{x})$ of the lensed radio source $[\vec{x} = (x, y)$ are coordinates on the sky], we then calculate (i) the radial component $v_r(\vec{x})$ of the velocity vector of the HI gas, where the line-of-sight pierces the disk, and (ii) the optical depth $\tau(\vec{x})$ for the sight line normal to the disk, which is then multiplied by $\cos(i)^{-1}$ to include the effect of inclination. We assume that the HI absorption line is isotropically (Gaussian) broadened by $\sigma_{\text{HI}} (= \text{FWHM}/2.35)$, constant as a function of radius.

We re-normalize the flux-density of the source, $\int \Sigma_v(\vec{x}) d^2\vec{x}$, to unity. The observed line profile becomes a convolution of a Gaussian velocity profile with the un-broadened line-profile¹, i.e.:

$$I(v) = \left\{ e^{v^2/2\sigma_{\text{HI}}^2} \right\} \star \left\{ \int_{v=v_r(\vec{x})} \Sigma_v(\vec{x}) [1 - \tau(\vec{x})] d\vec{x} \right\} \quad (1)$$

which is unity in the case of no absorption. Images of the radio sources – even though they have a continuous mapping and surface brightness distribution – are always affected by the finite beam size. Hence, instead of using the MERLIN image of PKS1830–211 to model $\Sigma_v(\vec{x})$, we instead use the clean components². In this case the integral in Eq.1 is simply replaced by a sum over the clean components. The resulting absorption line profile should therefore more closely resemble the underlying line profile³ for the deconvolved radio image of PKS1830–211. The free parameters in our kinematic model are $\{i, \theta, v_s, \sigma_{\text{HI}}, \tau_0, \gamma\}$. We furthermore set $v_c = \sqrt{2} \times \sigma_{\text{DM}} = 266 \text{ km s}^{-1}$, which follows from the isothermal lens mass model (i.e. a dark-matter dispersion of $\sigma_{\text{DM}}=188 \text{ km s}^{-1}$; in agreement with Winn et al. 2002), $r_0 = 0''.5$ (arbitrary value but roughly the Einstein radius), and the kinematic center is set to the lens centers inferred from the different authors discussed in Sect. 1. We register the optical and radio data, associating the bright radio cores with the optical quasar images.

4. RESULTS

Constraints on the kinematic model are the following: (i) the WSRT HI line-profile with 238 channels with

¹ This is correct only if the σ_{HI} is not a function of \vec{x} and note also that the Gaussian is not normalized.

² Clean components are delta functions with finite flux that, convolved with a Gaussian beam, reproduce the radio map as presented in Fig.1. In total our model of the source brightness distribution includes 350 clean components.

³ The line-width σ_{HI} might increase slightly because of unaccounted for minor velocity gradients between clean components.

3.9 km s^{-1} width each, with an average $1-\sigma$ measurement error of 0.00147 (Fig.2; three channels are removed due to band-pass edge uncertainties), and (ii) the velocity difference between components A and B of $147(\pm 1) \text{ km s}^{-1}$ (Wiklind & Combes 1998). We minimize χ^2 – as commonly defined – using a Downhill Simplex method with simulated annealing (Press et al. 1992), varying all six free parameters simultaneously.

We only explore models where the kinematic centers have been fixed at positions (notably often mutually exclusive) as previously published in the literature. Given degeneracies in the kinematic model, the current spatially unresolved line-profile and potential other issues (see below), we feel that a more sophisticated kinematic model is at this point not warranted.

The results are listed in Table 1. A number of conclusions can be drawn:

(1) The inclination of the HI disk, $i = (17 - 32)^\circ \pm 2^\circ$ ($1-\sigma$), is robust and nearly independent from the assumed kinematic center of the lens galaxy. This confirms that the lens galaxy is most likely a close-to face-on spiral galaxy, as previously proposed (e.g. Winn et al. 2002).

(2) The position angle of the disk varies between $\theta = +34^\circ$ and -15° . This result is clearly less robust than the inclination angle, due to degeneracies with the inclination and kinematic center.

(3) The line-width, $\sigma_{\text{HI}} = (39 - 48) \pm 1 \text{ km s}^{-1}$, is also robust. The value appears high compared with local spiral galaxies and might be the result of increased star formation, stirring up the HI gas to higher turbulent velocities. The line-width of molecular gas is also relatively high, $\sim 30 \text{ km s}^{-1}$ (Wiklind & Combes 1996). Even though lower than what we infer, such difference can be expected between colder molecular gas, presumably in clouds, and HI in the atomic (versus molecular) phase. However, the use of clean components to represent the, in reality, smooth Einstein Ring could somewhat broaden the fitted line-width because they undersample the velocity field (i.e. the field in between clean components will show a velocity gradient that is not sampled). The spectral resolution is negligible.

(4) The optical depth varies considerably as a function of radius for some of the models, with typical $1-\sigma$ statistical errors on τ_0 of ± 0.01 . In particular the models with the lens centers from Winn et al. (2002), Kochanek & Narayan (1992) and Courbin et al. (2002; only for model Sp) seem to prefer steeply *rising* optical depths as a function of radius (i.e. $\gamma \gg 0$). The other models also prefer rising optical depths, but more moderately. All models give a considerable HI depletion toward the lens center, as is also seen in some local galaxies, which could be the result of strong past and ongoing star formation (see also –3– above). This depletion can already be inferred from the fact that, even though image B is closer the inferred lens centers, it experiences less HI absorption (Fig.2).

(5) Plotting $\tau(r)$, we find that all models give $\tau \approx 0.085$ at $r = 5.0 h_{70}^{-1} \text{ kpc}$ along the disk, except for the lens center (Sp) from Courbin et al. (2002) for which 0.06 is found. However, from a lensing perspective it is unlikely that the latter position is that of the dominant

lens galaxy. The HI column density is $N_{\text{HI}} = 4.6 \times 10^{21} (T_s/100 \text{ K}) (\sigma_{\text{HI}}/\text{km s}^{-1}) \tau \text{ cm}^{-2}$ (given our definition of the line profile in Eq. 1). Assuming a “canonical” value of the unknown spin temperature of $T_s = 100 \text{ K}$, as in Chengalur et al. (1999), $\tau \approx 0.085$ at a radius of $5 h_{70}^{-1} \text{ kpc}$ in the disk and $\sigma_{\text{HI}} \approx 44 \text{ km s}^{-1}$, we find $N_{\text{HI}} \approx 2 \times 10^{21} \text{ cm}^{-2}$, similar to what was already found by Chengalur et al. and also similar to that of local spiral galaxies and damped Ly α systems.

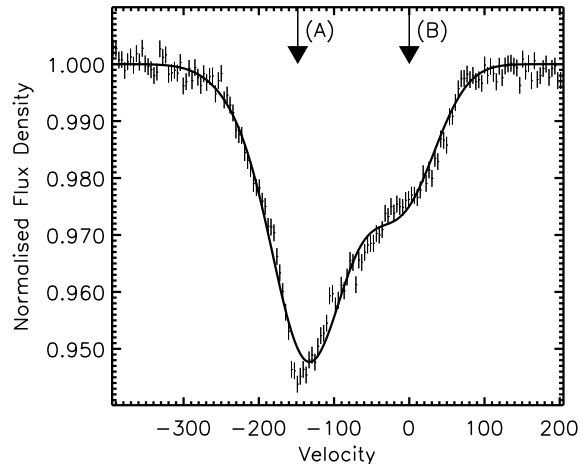


FIG. 2.— The WSRT HI-line profile overplotted with the best-fit kinematic model from Fig.1. Errors are 0.00147 in normalised units. The velocity is in units of km s^{-1} . A and B indicate the velocity positions of the two lensed cores of source.

We note that the range of parameter values are typically larger than their $1-\sigma$ errors, since the former reflects the change as function of chosen kinematic center.

The results have to be seen in light of some additional cautionary notes: First, we see that the χ^2 values are ~ 2 times the $\text{DOF}=229$. This is mostly due to a mismatch between the model and the observed HI line around A and B (see Fig.2). The lensed core of the source, however, is known to be time-variable (Lovell et al. 1998). Since, the MERLIN and WSRT data set were not obtained at exactly the same epoch (5 months in between), this might explain the mismatch. WSRT data from different epochs (not presented here) indeed show some minor differences between the observed HI lines.

Second, our models are azimuthally symmetric and assume an HI covering factor of 100%. If the HI column density (i.e. optical depth) is a function of angle along the disk, it could change the inferred kinematic results. Even though we believe the effect to be small, it can not fully be excluded. A spatially resolved HI absorption line profile would help to eliminate this possibility.

Third, we have assumed the 1.4-GHz maps to be a reasonable representation of the 0.75-GHz continuum structure of the lensed source, as discussed previously. If the spectral index is a strong function along the lensed source, it might also affect the results.

Fourth, we have assumed that the rotation curve of the spiral galaxy is flat. This is consistent with observations of local spiral galaxies with similar rotation velocities, but might not be a correct assumption for a galaxy at $z = 0.89$. Again, a spatially resolved HI absorption line profile would be able to test this assumption.

x_k (")	y_k (")	i (°)	θ (°)	σ_{HI} (km s ⁻¹)	γ	τ_0	χ^2	Reference
+0.532	-0.420	30	-15	40	0.76	0.076	443	Nair et al. (1993)
+0.519	-0.511	17	+23	48	0.65	0.078	446	Courbin et al. (2002), G
+0.500	-0.450	32	-15	39	0.66	0.079	443	Lehar et al. (2000)
+0.350	-0.510	17	+28	48	2.14	0.065	446	Kochanek & Narayan (1992)
+0.328	-0.486	20	+11	47	3.62	0.057	449	Winn et al. (2002)
+0.285	-0.722	21	+34	48	1.73	0.049	449	Courbin et al. (2002), Sp

Table 1 — Best-fits parameters of the kinematic models (see Sect. 3–4, also for errors).

5. DISCUSSION & CONCLUSIONS

We have modeled the neutral hydrogen (HI) distribution and kinematics in the spiral galaxy of the lens system PKS 1830–211 at $z=0.89$, using a MERLIN 1.4-GHz continuum map of the Einstein ring and an WSRT HI absorption line. The main numerical results are summarized in Sect. 4.

In general, we find that the HI disk is seen close-to face-on, as previously suggested (e.g. Winn et al. 2002). We find evidence for HI depletion toward the galaxy center and a column density of $N_{\text{HI}} \approx 2 \times 10^{21} \text{ cm}^{-2}$ at $5 h_{70}^{-1} \text{ kpc}$, comparable to those of low redshift spiral galaxies. Our data are insufficient to discriminate between the different lens centers as published by different authors and we have to await new HST–ACS observations.

We emphasize some cautionary notes, listed in Sect. 4, regarding our results. Even so, we believe that our analysis is a good first attempt to constrain the kinematics of neutral hydrogen in a spiral galaxy at relatively high redshift, within the current observational limits, and should be regarded as such.

Our analysis shows that the combination of HI observations with gravitational lensing – in particular radio Einstein rings – potentially provide a strong tool to study spiral galaxies to high redshifts. A similar program to combine lensing and stellar kinematics of E/S0 galaxies out to $z \sim 1$ is currently underway (i.e. the Lenses Structure & Dynamics (LSD) Survey; e.g. Koopmans & Treu 2002, 2003; Treu & Koopmans 2002).

We anticipate that *spatially resolved* HI absorption line

profiles and radio continuum images at the redshifted HI-line frequency can be obtained of many similar systems in the future with e.g. ALMA, LOFAR and SKA. This would resolve many of the issues outlined in the paper and provide us with an unprecedented probe into the internal structure of spiral galaxies at high redshifts. By probing spiral lenses over a range of redshifts, their evolution can be studied (e.g. Koopmans & de Bruyn 1999), providing a complementary tool to study spiral galaxies between those at low redshifts using HI emission and damped Ly- α systems at very high redshifts.

We note, however, that none of the other studies can provide *two independent* constraints, i.e. from lensing and kinematics, on the same mass distribution of the spiral galaxy. Their combination can break degeneracies inherent to each technique separately. Our results, admittedly based on a single system, show that very interesting constraints can be obtained for spiral galaxies at high redshifts.

We like to thank Tom Muxlow for doing the initial calibration of the MERLIN data. We also thank Eric Agol, Ron Allen, Mike Fall and Mario Livio for comments and discussions. LVEK acknowledges the support from an STScI Fellowship grant. MERLIN is a National Facility operated by the University of Manchester at Jodrell Bank Observatory on behalf of PPARC. The Westerbork Synthesis Radio Telescope (WSRT) is operated by the Netherlands Foundation for Research in Astronomy (ASTRON) with the financial support from the Netherlands Organisation for Scientific Research (NWO).

REFERENCES

- Chengalur, J. N., de Bruyn, A. G., & Narasimha, D. 1999, A&A, 343, L79
 Courbin, F., Meylan, G., Kneib, J.-P., & Lidman, C. 2002, ApJ, 575, 95
 Gerin, M., Phillips, T. G., Benford, D. J., Young, K. H., Menten, K. M., & Frye, B. 1997, ApJ, 488, L31
 Jauncey, D. L. et al. 1991, Nature, 352, 132
 Kauffmann, G. 1996, MNRAS, 281, 475
 Kochanek, C. S. & Narayan, R. 1992, ApJ, 401, 461
 Koopmans, L. V. E. & Treu, T. 2003, ApJ, 583, 606
 Koopmans, L. V. E. & Treu, T. 2002, ApJ, 568, L5
 Koopmans, L. V. E., & de Bruyn, A. G., 1999, in Perspectives on Radio Astronomy: Science with Large Antenna Arrays, ed. M. P. van Haarlem, p213
 Lehar, J. et al. 2000, ApJ, 536, 584
 Lidman, C., Courbin, F., Meylan, G., Broadhurst, T., Frye, B., & Welch, W. J. W. 1999, ApJ, 514, L57
 Lovell, J. E. J., Jauncey, D. L., Reynolds, J. E., Wieringa, M. H., King, E. A., Tzioumis, A. K., McCulloch, P. M., & Edwards, P. G. 1998, ApJ, 508, L51
 Mathur, S. & Nair, S. 1997, ApJ, 484, 140
 Mo, H. J., Mao, S., & White, S. D. M. 1998, MNRAS, 295, 319
 Nair, S., Narasimha, D., & Rao, A. P. 1993, ApJ, 407, 46
 Pramesh Rao, A. & Subrahmanyam, R. 1988, MNRAS, 231, 229
 Press, W. H., Teukolsky, S. A., Vetterling, W. T., & Flannery, B. P. 1992, Cambridge: University Press, 1992, 2nd ed.
 Shepherd, M. C. 1997, ASP Conf. Ser. 125: Astronomical Data Analysis Software and Systems VI, 6, 77
 Subrahmanyam, R., Narasimha, D., Pramesh-Rao, A., & Swarup, G. 1990, MNRAS, 246, 263
 Treu, T. & Koopmans, L. V. E. 2002, ApJ, 575, 87
 Wiklind, T. & Combes, F. 1996, Nature, 379, 139
 Wiklind, T. & Alloin, D., 2002, in Lecture Notes Phys. 608, 124
 Winn, J. N., Kochanek, C. S., McLeod, B. A., Falco, E. E., Impey, C. D., & Rix, H. 2002, ApJ, 575, 103